THE PENNSYLVANIA STATE UNIVERSITY
SCHREYER HONORS COLLEGE

DEPARTMENT OF METEOROLOGY AND ATMOSPHERIC SCIENCE

DIAGNOSING SUMMERTIME $PM_{2.5}$ BIASES OF THE COMMUNITY MULTISCALE AIR QUALITY MODEL

BENJAMIN YANG
FALL 2019

A thesis
submitted in partial fulfillment
of the requirements
for a baccalaureate degree
in Meteorology and Atmospheric Science
with honors in Meteorology and Atmospheric Science

Reviewed and approved* by the following:

Kenneth Davis
Professor of Atmospheric and Climate Science
Thesis Supervisor

Johannes Verlinde
Professor of Meteorology and Atmospheric Science
Honors Adviser

* Signatures are on file in the Schreyer Honors College.

ABSTRACT

Particulate matter with a diameter of 2.5 micrometers or less ($PM_{2.5}$) is one of the most harmful ambient air pollutants to human health. To improve regional air quality forecasting, it is essential to upgrade numerical weather prediction models. The Environmental Protection Agency's (EPA) Community Multiscale Air Quality (CMAQ) model is driven by two National Oceanic and Atmospheric Administration (NOAA) numerical weather predictions: the operational North American Mesoscale (NAM) model and the experimental Finite Volume Cubed-Sphere Global Forecasting System (FV3GFS) model. $PM_{2.5}$ predictions by both models were compared and evaluated over the contiguous United States (CONUS) from 1-19 June 2019, using AirNow observations. Aircraft-derived planetary boundary layer (PBL) height and surface weather station observations were compared against the corresponding predicted meteorology.

The FV3GFS-CMAQ generally predicted less $PM_{2.5}$ than the NAM-CMAQ in the eastern United States. Following a cold front passage over the Southeast, the NAM-CMAQ overpredicted $PM_{2.5}$, while the FV3GFS-CMAQ underpredicted $PM_{2.5}$. Similar divergences in $PM_{2.5}$ predictions occurred on other cold front days. Enhanced vertical mixing due to wind shear in the FV3GFS-CMAQ weakened the temperature inversion in the nocturnal boundary layer, allowing for warmer and drier air from aloft to be mixed down. Due to this enhanced vertical mixing, the FV3GFS-CMAQ likely overpredicted PBL height and dry deposition, thereby reducing surface $PM_{2.5}$ concentrations. The NAM-CMAQ probably has the preferred PBL scheme and resolution in our case study, as underprediction may cause greater $PM_{2.5}$ exposure. Horizontal advection and wet deposition are other important $PM_{2.5}$ removal mechanisms, which should be explored more extensively in future case studies over various regions and time periods.

TABLE OF CONTENTS

LIST OF FIGURES

ACKNOWLEDGEMENTS

I would like to express my sincere gratitude to Kenneth Davis and Johannes Verlinde for their exceptional mentorship throughout my academic and research endeavors at Penn State. Through Davis's group, I worked closely with Nikolay Balashov, who selflessly offered computer programming tips, and Sandip Pal, who provided invaluable insight about the planetary boundary layer. Thanks to the National Science Foundation and National Centers for Environmental Prediction for funding my incredible summer research experiences. Special thanks to Yunha Lee, Vikram Ravi, Joseph Vaughan, and Brian Lamb at the Laboratory for Atmospheric Research at Washington State University. It was through their guidance that I learned the intricacies of numerical weather prediction and air quality forecasting. Finally, this investigation would not have been possible without the generous support and advice from Jeff McQueen, Jianping Huang, and the rest of the air quality team at the NOAA Environmental Modeling Center.

Chapter 1

Introduction

Countless epidemiological studies worldwide have highlighted the link between particulate matter with an aerodynamic diameter of 2.5 micrometers or less ($PM_{2.5}$) and premature death from heart and lung disease. Elevated $PM_{2.5}$ concentrations also degrade visibility through haze, threaten ecosystems through acid rain, and contribute to regional and global aerosol-climate feedbacks. As part of the National Ambient Air Quality Standards (NAAQS), the primary and secondary standards for $PM_{2.5}$ over a 24-hour averaging period are both currently 35 $\mu g\ m^{-3}$ (EPA 2012). Deficiencies in air quality dispersion models must be identified to improve numerical simulations of $PM_{2.5}$ and forestall adverse impacts occurring on local, regional, and global scales (Zhang et al. 2015). While many studies have focused on simulating the atmospheric dispersion of pollutants in the daytime convective boundary layer, fewer studies have detailed dispersion processes during the nighttime or transition times on regional scales (Hu et al. 2013).

Primary sources of $PM_{2.5}$ include power plants, motor vehicles, wildfires, and dust storms, which all directly emit these fine particles. Additionally, precursor gases, such as sulfur dioxide, nitrogen oxides, ammonia, and volatile organic compounds, can undergo chemical reactions that lead to the secondary formation of $PM_{2.5}$ (Brook et al. 2007). Photochemical reactions of such precursor gases are sped up as temperature increases. A study conducted in Japan found a strong positive correlation between temperature and $PM_{2.5}$ concentration, which is

consistent with past investigations (Wang and Ogawa 2015). However, some researchers caution against the sole reliance on this relationship because high temperatures in the summer do not necessarily indicate higher ozone concentrations, especially when comparing cities, such as Philadelphia and Seattle, located in distinct climate zones (Greene et al. 1998).

Other conventional meteorological variables, including precipitation, humidity, wind speed, wind direction, and cloud cover, can influence $PM_{2.5}$ levels as well. Precipitation is negatively correlated with $PM_{2.5}$ concentration, whereas humidity is positively correlated with $PM_{2.5}$ under hygroscopic growth, but negatively correlated with $PM_{2.5}$ under dry deposition above a certain threshold (Wang and Ogawa 2015). Wang and Ogawa also found that wind speed is negatively correlated with $PM_{2.5}$ concentration below 3 m s^{-1}, but positively correlated above 3 m s^{-1}. It is important to consider wind direction, as pollutants can be horizontally advected from nearby or distant sources. Optically thick stratiform or cumuliform clouds scatter more incident solar radiation back to space, while optically thin cirrus clouds, typically associated with fair weather, absorb more outgoing longwave radiation (Mitchell and Finnegan 2009). Increased coverage of optically thick clouds not only limits photochemical reactions which lead to secondary $PM_{2.5}$ formation, but also suppresses planetary boundary layer (PBL) growth.

From an Eulerian framework, the depth of the convective boundary layer increases during the day, as vertical mixing occurs due to heat, moisture, and momentum fluxes. This mixing distributes pollutants through a greater depth. At night, a shallower layer, known as the stable or nocturnal boundary layer, traps pollutants near the surface, although vertical transport associated with a “leaky” residual layer can occur (Hu et al. 2012). Both horizontal advection and vertical mixing of $PM_{2.5}$ are important removal mechanisms. Contrary to previous proposals, a recent study found that vertical mixing was not as significant in the context of cold air

outbreaks in northern China (Liu et al. 2019). A study focused on a nocturnal cold front passage in Oklahoma in April 2016 found that there was enhanced vertical mixing and dry deposition of ozone in the Weather and Research Forecasting Model coupled with chemistry (WRF-Chem). In unstable environments, heavy convective showers are often associated with cold front passages. While wet deposition efficiency greatly depends on rainfall intensity and particle diameter, wet deposition in Beijing during the summer was found to constitute 92% of the $PM_{2.5}$ removal (Wu et al. 2018). Therefore, it is essential to consider whether synoptic patterns involve precipitation and to examine the relative contribution of precipitation to $PM_{2.5}$ removal.

Since January 2015, the NOAA-EPA National Air Quality Forecasting Capability (NAQFC) has provided real-time developmental 48-hour $PM_{2.5}$ forecasts at 06 UTC and 12 UTC over the United States to state and regional air quality forecasters (Huang et al. 2017). Upgrades in 2015 included the addition of windblown dust emissions, which improved PM predictions in the western United States, and the suppression of fugitive dust, which reduced PM bias by 52% in the northern-central United States (Lee et al. 2016). With the North American Mesoscale (NAM) model driving operational Community Multiscale Air Quality Model (CMAQ) forecasts, summertime underprediction of $PM_{2.5}$ has prevailed, possibly due to archaic emission inventories and intense wildfire activity (Huang et al. 2017). In addition to the NAM, NOAA has used the Finite Volume Cubed-Sphere Global Forecasting System (FV3GFS) dynamical core to drive experimental CMAQ predictions. In general, summertime $PM_{2.5}$ of the FV3GFS-CMAQ has been underpredicted over the eastern United States, which may be due to overpredicted PBL heights and overmixing of $PM_{2.5}$ (Huang et al. 2018). To our knowledge, this investigation is the first to formally link the dynamics of a nocturnal cold front passage with these summertime $PM_{2.5}$ prediction biases.

The primary objective of this study was to analyze how the prediction biases of different meteorological parameters—wind speed, temperature, relative humidity, and PBL height—are attributed to $PM_{2.5}$ biases, particularly in the context of a nocturnal cold front passage. We first compared daily and hourly $PM_{2.5}$ prediction biases of the NAM-CMAQ and FV3GFS-CMAQ over the contiguous United States (CONUS) during June 2019. Thereafter, we identified a specific region and time period of greatest divergence in $PM_{2.5}$ bias between the NAM-CMAQ and FV3GFS-CMAQ. A case study of the relationships among the $PM_{2.5}$ and meteorological prediction biases allowed for an in-depth discussion of the relative importance of distinct $PM_{2.5}$ removal mechanisms, namely horizontal advection, vertical mixing, and wet deposition. Given past speculations of the greater mixing in the FV3GFS-CMAQ relative to the NAM-CMAQ, we hypothesized that vertical mixing was the predominant removal mechanism.

Chapter 2

Data and Methods

2.1 Model Descriptions

Offline coupling between the EPA's CMAQ version 5.0.2 and each of NOAA's two meteorological drivers were used to evaluate the impact of the numerical weather prediction output on $PM_{2.5}$ predictions. This version of the CMAQ incorporates the Carbon-Bond 2005 (CB05) gas-phase chemical mechanism, National Emission Inventory with base year 2014 (NEI2014), Biogenic Emission Inventory System (BEIS3), aerosol module (AERO6), and Hazard Mapping System (HMS) fire products (Huang et al. 2017). The North American Mesoscale (NAM) Nonhydrostatic Multiscale Model with Arakawa B-grid staggering (NMMB) with 12-km horizontal resolution and 35 vertical hybrid sigma levels was compared with the Finite Volume Cubed-Sphere Global Forecasting System (FV3GFS) with 13-km horizontal resolution and 64 vertical hybrid sigma levels. Air quality predictions differed partly from the treatment of boundary layer mixing, as the NAM has a high-order local turbulent kinetic energy PBL scheme, while the FV3GFS has an eddy-diffusivity mass-flux PBL scheme. Figure 1 illustrates the components of the NAQFC, with the FV3GFS as the meteorological driver.

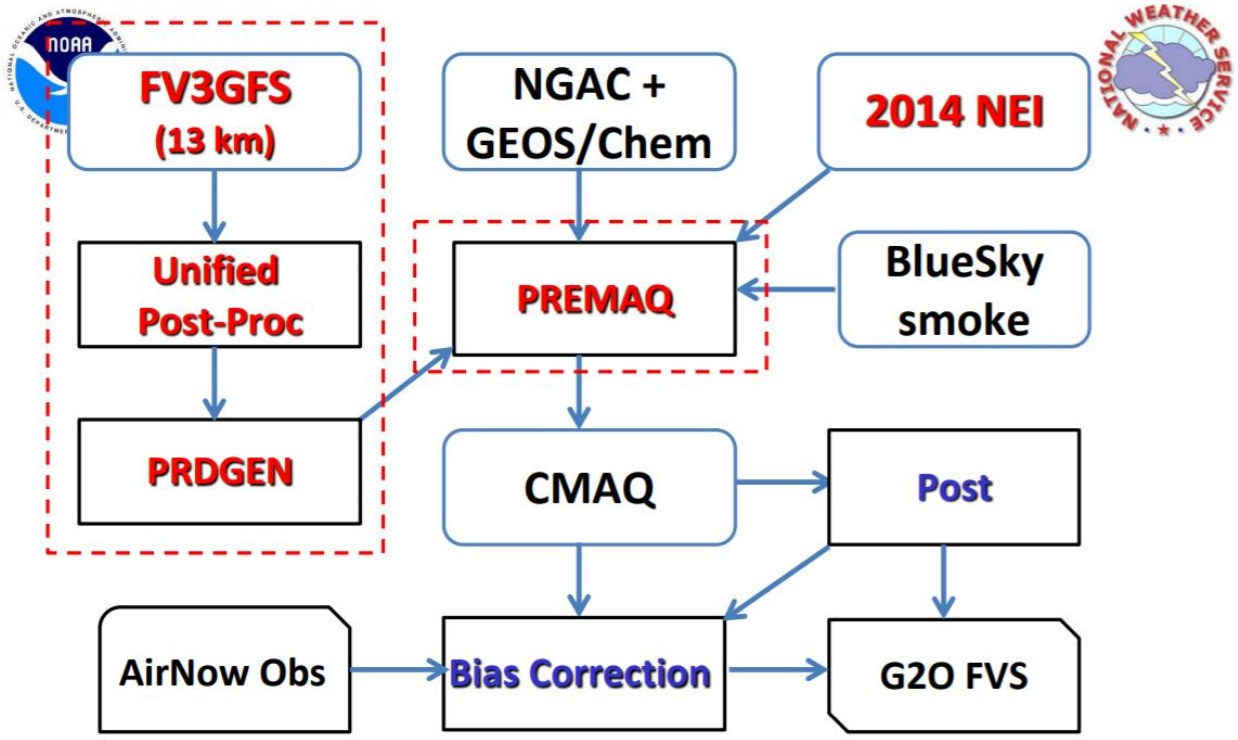

Figure 1. Flow chart of the FV3GFS-CMAQ system, taken from Huang et al. 2018. The red dashed boxes indicate recent changes to the system, as of October 2018. Offline coupling between the FV3GFS and CMAQ is achieved through the Unified Post-Processing System, pre-processors PRDGEN and PREMAQ, NOAA Environmental Modeling System GFS Aerosol Component (NGAC), Goddard Earth Observing System (GEOS) model with chemistry, 2014 NEI, and BlueSky smoke framework. Following post-processing and bias correction, dependent on AirNow observations, the Forecast Verification System (FVS) grid2obs tool can be used.

Considering that the FV3GFS-CMAQ only accounts for wildfire emissions, a time period without significant wildfire smoke affecting the CMAQ domain was selected, 1-19 June 2019. Anthropogenic emissions, agricultural activity, and dust were relevant sources of $PM_{2.5}$. For both models, daily 24-hour average $PM_{2.5}$ (4 UTC to 4 UTC) output files were extracted from NOAA Environmental Modeling Center runs. Furthermore, subsets of 48-hour forecasts initialized daily only at 12 UTC were used. Model output variables include near-surface $PM_{2.5}$ (level 1), surface pressure, 2-m air temperature, 2-m water vapor mixing ratio, 10-m wind speed, and PBL height

(based on the Richardson number). To estimate 2-m relative humidity, an algorithm provided by Zelle (2012) was employed, based on the formula

$$(RH)_2 = q_2 \cdot \left(\frac{a_1}{p_0}\right)^{-1} \cdot \left\{\exp\left[\frac{a_2(T_2 - a_3)}{(T_2 - a_4)}\right]\right\}^{-1} \cdot 100 \qquad (1)$$

where $(RH)_2$ is the approximate 2-m relative humidity (%), q_2 is the 2-m water vapor mixing ratio (kg kg^{-1}), p_0 is the surface pressure (Pa), T_2 is the 2-m air temperature (K), and a_1, a_2, a_3, and a_4 are constants.

2.2 Model Evaluations

$PM_{2.5}$ observations were obtained from 969 total possible monitoring sites across the EPA's AirNow network using the AirNow application programming interface (API) (AirNow 2019). Similarly, temperature, relative humidity, and wind speed observations were taken from 2,030 total possible stations from the National Weather Service's Automated Surface Observing System network using the Synoptic Data Mesonet API and Python package MesoPy (Synoptic Data 2019). PBL height measurements were acquired from 312 total possible Aircraft Communication Addressing and Reporting System (ACARS) commercial flights (Tsidulko et al. 2011). The number of available observations, especially PBL height, varied by day and region. Python programs were designed for the data analysis process, which included procedures for finding the nearest grid cell to a given station and closest instantaneous observation to a given hour.

CONUS maps of daily predicted 24-hour average $PM_{2.5}$ and $PM_{2.5}$ bias were generated from 1-19 June 2019. Averaging over all AirNow sites, time series were produced to show the daily variation of predicted 24-hour average $PM_{2.5}$ and $PM_{2.5}$ bias. The mean bias, a simple and commonly used metric for model evaluation, is the difference between predicted and observed values and is represented as

$$B_{MB} = \frac{1}{N}\sum_{i=1}^{N}(P_i - O_i) = \bar{P} - \bar{O} \qquad (2)$$

where B_{MB} is the mean $PM_{2.5}$ model bias, $\bar{P}$ is the predicted $PM_{2.5}$ concentration, $\bar{O}$ is the observed $PM_{2.5}$ concentration, and N is the number of functional AirNow sites. The main criteria in choosing a unique case study consisted of relatively high $PM_{2.5}$ bias for both models and a divergence in $PM_{2.5}$ bias between the two simulations. By narrowing the time frame and study area, the intricacies of atmospheric dispersion were closely examined.

2.3 Case Study Synopsis

Our case study is a cold front passage that traversed the southeastern United States from 10-11 June 2019. Spatial maps, time series plots, and Hovmöller diagrams were created to illustrate the overall divergence in $PM_{2.5}$ bias and hourly evolution of $PM_{2.5}$ bias. Using routine surface analysis maps from the Weather Prediction Center (WPC 2019), the synoptic features associated with this case study became more transparent. Beginning at 12 UTC on 10 June 2019, 48-hour predictions of $PM_{2.5}$, wind speed, temperature, relative humidity, and PBL height were

plotted versus forecast hour. Again, Equation (2) was used to calculate the model biases, but for each of the aforementioned parameters. Because the biases were averaged over the entire study region, we discuss the case study results more qualitatively in Chapter 3.

Chapter 3

Results and Discussion

3.1 CONUS Maps

As displayed in Figure 2, both models generally overpredicted $PM_{2.5}$ in the Pacific Northwest and Midwest and underpredicted $PM_{2.5}$ in California and the Gulf Coast states from 1-19 June 2019. Over much of the eastern United States, the FV3GFS-CMAQ predicted lower $PM_{2.5}$ concentrations relative to the NAM-CMAQ, which is desirable in areas of overprediction, but undesirable in areas of underprediction.

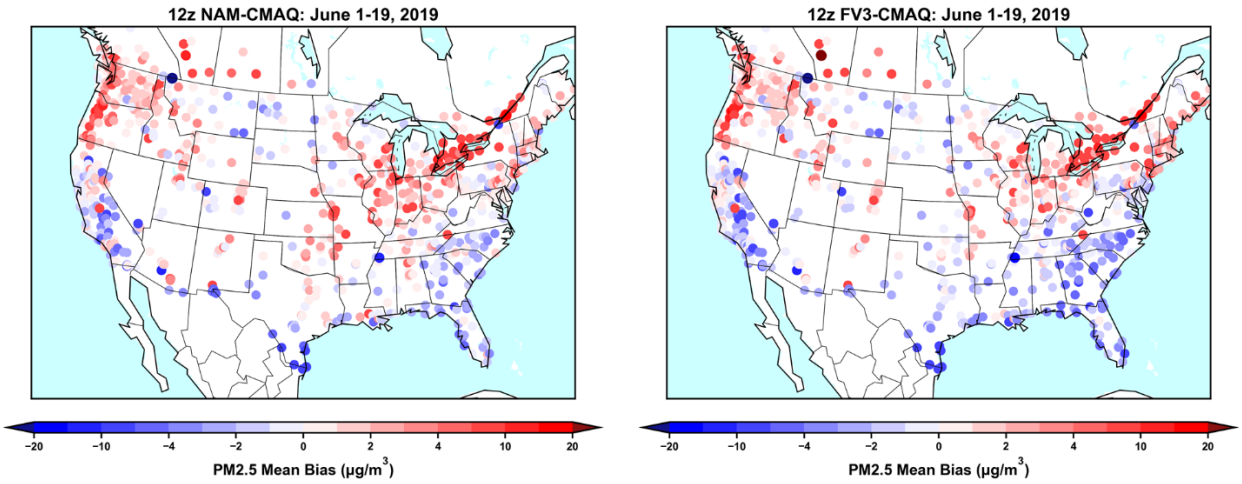

Figure 2. Overall daily 24-hour average $PM_{2.5}$ biases (predicted minus observed) of the NAM-CMAQ (left) and FV3GFS-CMAQ (right). Hourly $PM_{2.5}$ concentrations were averaged from 4 UTC on one day to 4 UTC on the next day. The biases were averaged from 1-19 June 2019. Each point represents an AirNow site, with darker/larger blue points representing greater underprediction and darker/larger red points representing greater overprediction.

Note that a particular location, such as in northwest Montana, with unusually large $PM_{2.5}$ bias could be due to instrumentation problems causing unreliable observations at the given AirNow site. Errors in $PM_{2.5}$ emissions, chemistry, or deposition are possible where the NAM-CMAQ and FV3GFS-CMAQ biases are similar. For example, biogenic volatile organic compounds, such as isoprene, play key roles in secondary organic aerosol formation contributing to the total $PM_{2.5}$, which could be mispresented in the vegetated Southeast (Weber et al. 2017). However, this study is primarily concerned with areas where NAM-CMAQ and FV3GFS-CMAQ biases differ, which reveal discrepancies between the two numerical weather models.

Spatial maps of daily predicted 24-hour average $PM_{2.5}$ concentrations indicate that $PM_{2.5}$ levels largely remained below the NAAQS of 35 µg m^{-3} over the CONUS domain from 1-19 June 2019. Figure 3 shows that the $PM_{2.5}$ levels of both the NAM-CMAQ and FV3GFS-CMAQ were visibly below the NAAQS in the United States on 11 June 2019.

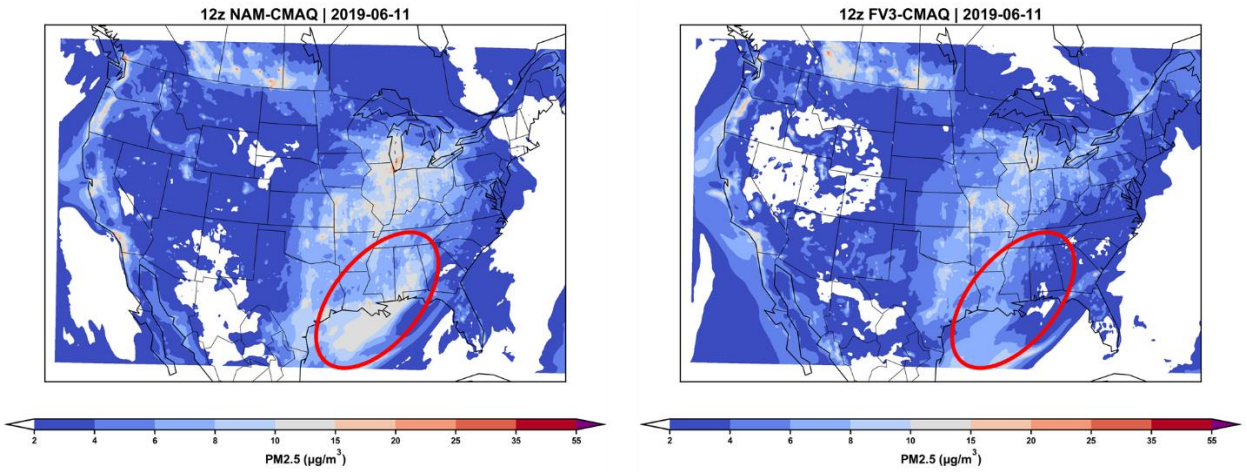

Figure 3. Daily 24-hour average $PM_{2.5}$ concentrations of the NAM-CMAQ (left) and FV3GFS-CMAQ (right) for 11 June 2019. White and darker blue indicate lower $PM_{2.5}$ concentrations, while red and purple indicate higher $PM_{2.5}$ concentrations (above NAAQS). The red ovals delineate an area of large $PM_{2.5}$ difference.

Both models show several urban areas with relatively high $PM_{2.5}$ concentrations, particularly along the West Coast and in the Midwest. There is broader coverage of modest $PM_{2.5}$ levels of 4-15 μg m^{-3} in the eastern United States in both models, which signifies the role of atmospheric dispersion and synoptic weather patterns. Major wildfire smoke affecting CONUS is unlikely on 11 June, as we would expect $PM_{2.5}$ levels to greatly exceed the NAAQS. Although we noticed higher $PM_{2.5}$ levels associated with dust intrusion off the coast of Florida late in the period, anthropogenic activity appears to be the main source of $PM_{2.5}$ in this case study.

3.2 Case Study Region: Southeast

A prominent swath of elevated $PM_{2.5}$ levels in the red circled area for the NAM-CMAQ is absent over the same area for the FV3GFS-CMAQ (Figure 3). After finding this difference, we noticed a spatially coincident swath of large negative $PM_{2.5}$ difference, shaped as the downstream portion of an upper-level trough (Figure 4). The magnitudes of these differences are as high as 10-15 μg m^{-3} and are fairly continuous within the swath. The black box drawn around the portion of this swath over land is our case study region, which we will also refer to as the "Southeast." This study region includes highly populated cities such as Atlanta, Birmingham, Memphis, New Orleans, and Tallahassee.

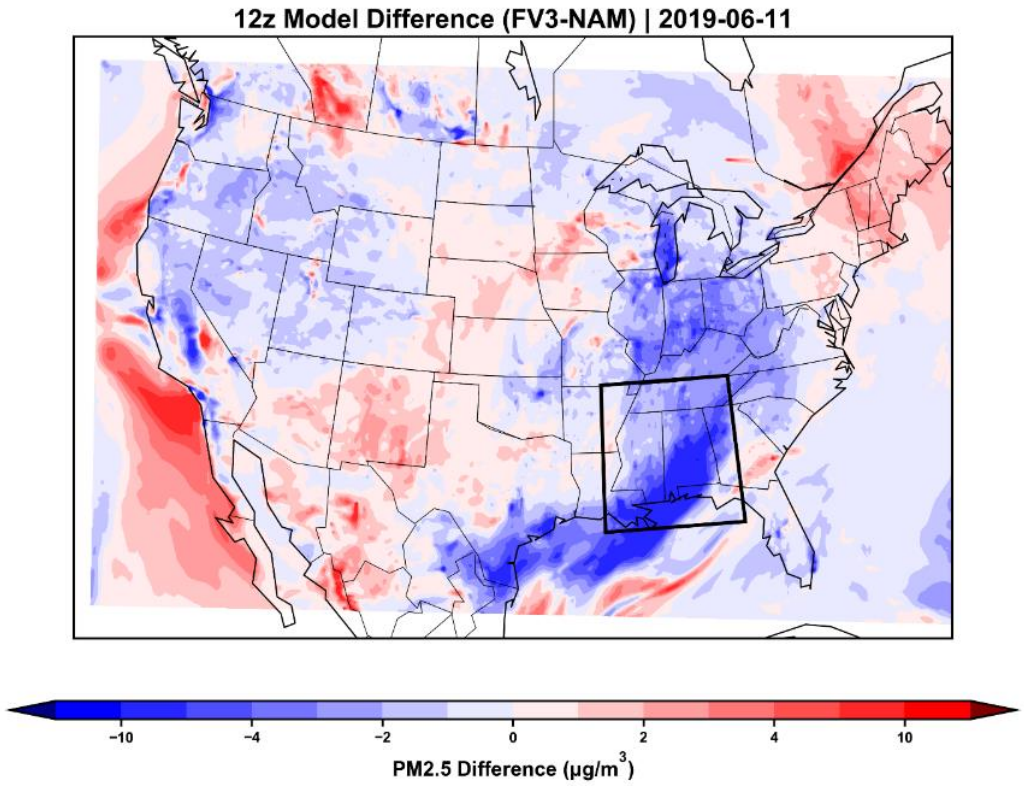

Figure 4. Differences in predicted 24-hour average $PM_{2.5}$ concentrations on 11 June 2019 (FV3GFS-CMAQ minus NAM-CMAQ). Blue indicates a negative difference, while red indicates a positive difference. The box represents our study area.

3.3 Cold Front Passage: 10-11 June 2019

From 10-11 June 2019, a well-established cold front traversed the Southeast. Figure 5 shows the cold front at 03 UTC on June 11 and convective precipitation ahead of the cold front. Although wet deposition could have occurred at this time, a series of surface analysis maps from 10-11 June show heavy, isolated, and short-lived showers. Thus, higher model resolution is preferable to capture the mesoscale details of these showers. The NAM's horizontal resolution is only 1 km higher than that of the FV3GFS, which suggests that differences in predicted precipitation alone cannot explain the large differences in $PM_{2.5}$.

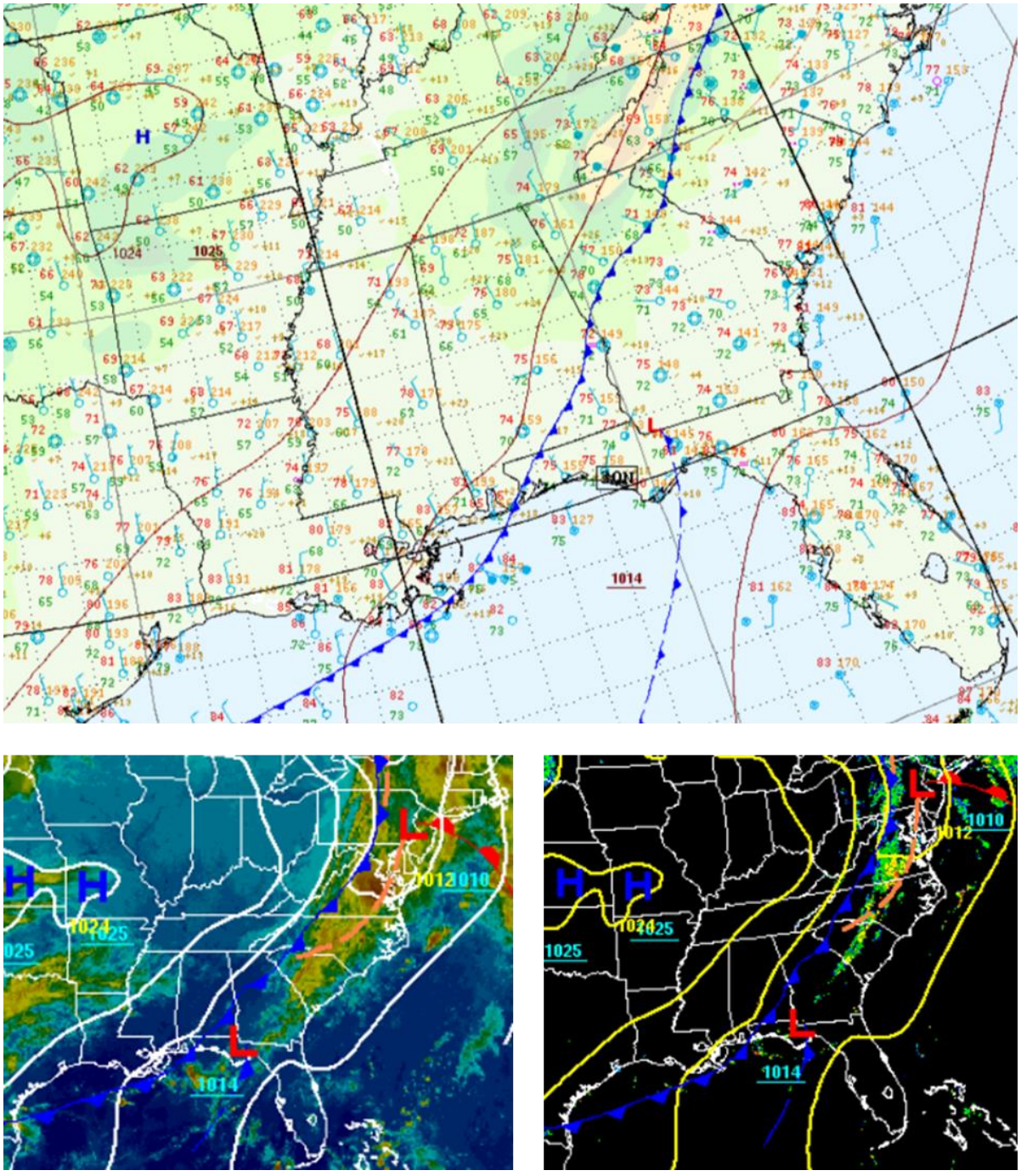

Figure 5. Surface analysis maps at 03 UTC on 11 June 2019 from the Weather Prediction Center. A cold front traversing the Southeast is outlined using the station models and NAM topography (top), infrared satellite composite (bottom left), and radar composite (bottom right).

3.4 Divergence in $PM_{2.5}$ Predictions

To contextualize this case, Figure 6 highlights a marked divergence in $PM_{2.5}$ and $PM_{2.5}$ bias between the NAM-CMAQ and FV3GFS-CMAQ on 11 June. The NAM-CMAQ overpredicted $PM_{2.5}$, while the FV3GFS-CMAQ underpredicted $PM_{2.5}$ on this day. Similarly, divergences in bias, albeit less prominent, occurred on 3 and 13 June. Cold fronts traversed the Southeast on these days as well, which suggests that cold fronts may be linked with $PM_{2.5}$ bias divergences. Note that both the NAM-CMAQ and FV3GFS-CMAQ biases dipped on 16 June, which was a high-pressure day, likely as a result of non-meteorological factors such as emissions or chemistry errors. We suspect that model initialization issues caused the large biases from around 1-5 June; therefore, the correlation coefficients are not accurate over the entire period. Neglecting these days when the FV3GFS-CMAQ underperformed, the FV3GFS-CMAQ appears to have outperformed the NAM-CMAQ.

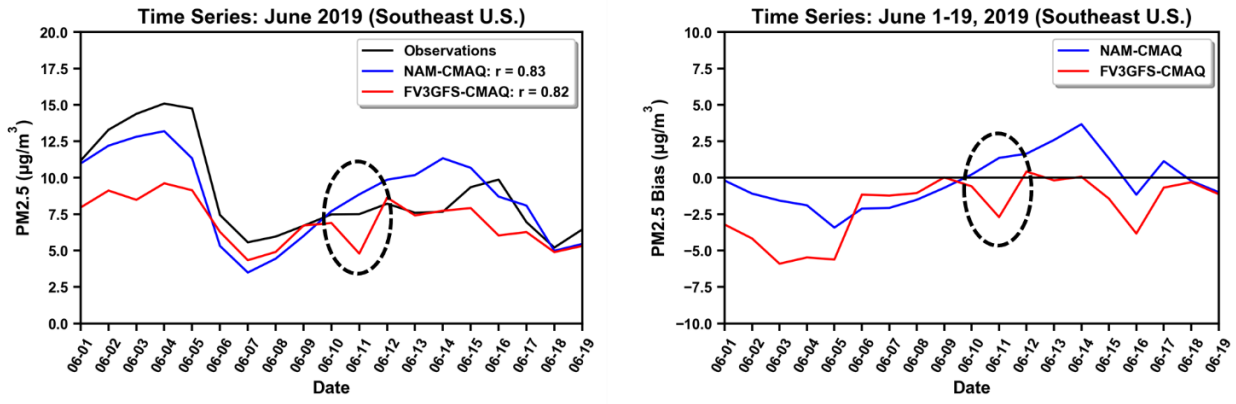

Figure 6. Time series of daily 24-hour average $PM_{2.5}$ (left) and $PM_{2.5}$ bias (right) over the Southeast. The blue lines represent the NAM-CMAQ, the red lines represent the FV3GFS-CMAQ, and black lines either represent observations (left) or no bias (right). Black dotted ovals surround the divergence of interest for our case study.

3.5 Meteorological Influences

Referring to Figure 7, we attempt to diagnose the primary cause of the $PM_{2.5}$ bias divergence on 11 June using hourly time series of $PM_{2.5}$ bias and bias of meteorological parameters, including wind speed, temperature, relative humidity, and PBL height. Starting at 12 UTC on 10 June, the $PM_{2.5}$ biases of the NAM-CMAQ and FV3GFS-CMAQ roughly overlap one another. From around 18 UTC on 10 June to 03 UTC on June 11 (forecast hours 6-15), when the cold front moved through the study region, the $PM_{2.5}$ biases separate increasingly. For the rest of the forecast period, the spacing between the NAM-CMAQ $PM_{2.5}$ overprediction and FV3GFS-CMAQ underprediction remain roughly constant.

During the transition time (purple area in Figure 7), both the NAM-CMAQ and FVGFS-CMAQ had increases in wind speed bias, but the FV3GFS-CMAQ wind speed bias increased to a greater extent. There may have been stronger wind shear in the FV3GFS-CMAQ, which led to overmixing and $PM_{2.5}$ underprediction. Spatial maps of FV3GFS-CMAQ $PM_{2.5}$ indicate that the prevailing winds advected $PM_{2.5}$ from areas of higher $PM_{2.5}$ concentrations to areas of lower $PM_{2.5}$ concentrations. Thus, horizontal advection may have been a smaller factor than vertical mixing in the $PM_{2.5}$ bias divergence. This would be consistent with the study by Hu et al. (2013), which explains that stronger wind shear enhanced turbulent mixing in the WRF-Chem during a nocturnal cold front passage in Oklahoma.

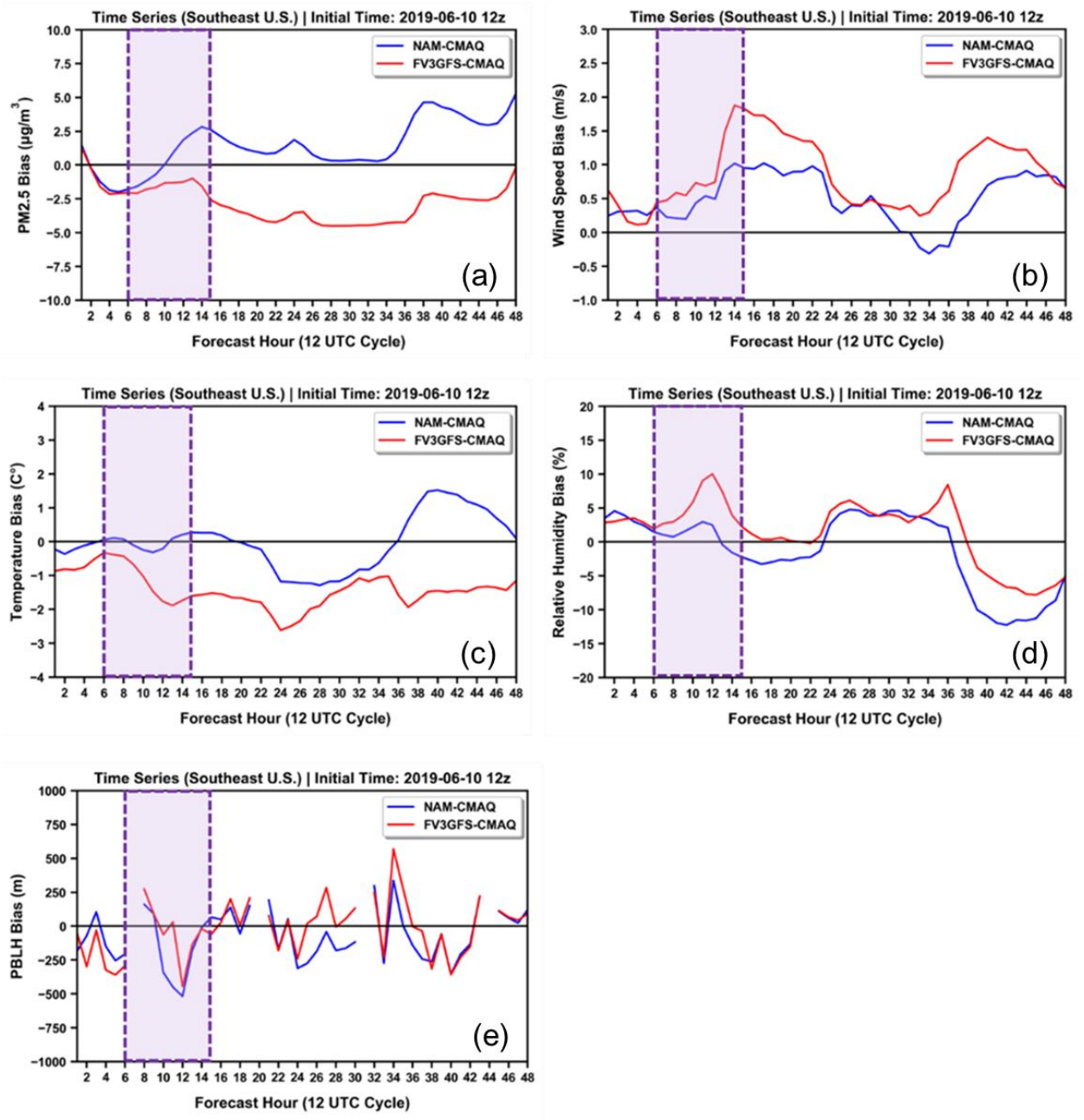

Figure 7. Hourly time series of $PM_{2.5}$ bias (a), wind speed bias (b), temperature bias (c), relative humidity bias (d), and PBL height bias (e) from 12 UTC on 10 June to 12 UTC on 12 June. Blue lines (NAM-CMAQ) and red lines (FV3GFS-CMAQ) are compared. The purple shaded areas approximate the cold front passage.

Turbulent vertical mixing as a result of wind shear weakened the temperature inversion in the nocturnal boundary layer, allowing for warmer air from aloft to be mixed down to the surface. As evident in Figure 7, the temperature bias of both models increased for a few hours during and after the cold front traversed the region. Yet, the FV3GFS-CMAQ temperature bias decreased more noticeably as the cold front traversed the region, possibly reducing the secondary formation of $PM_{2.5}$. The FV3GFS-CMAQ relative humidity bias had a greater peak due to enhanced mixing ahead of the front in the moist warm sector. Behind the front in the cold sector of the low-pressure system, drier air from aloft was mixed down, more excessively in the FV3GFS-CMAQ. This is indicated by a sharper decline in relative humidity bias. Enhanced precipitation, thus more wet deposition, may have also contributed to the underprediction in the FV3GFS-CMAQ, but it was probably not the overarching factor.

As vertical mixing increases, PBL height and the volume in which particles are mixed increase, thus decreasing $PM_{2.5}$ concentration. Figure 7 shows that the FV3GFS-CMAQ underpredicted PBL height during the transition time, but to a lesser extent than the NAM-CMAQ. Sparse, inconsistent PBL height observations limit the reliability of our results, and missing PBL height observations explain the gaps in the predicted PBL height biases. Figure 8 displays the vertical distribution of $PM_{2.5}$ in the lowest 5 km of the atmosphere for both models. While $PM_{2.5}$ concentrations increased in the NAM-CMAQ during the transition time, they decreased in the FV3GFS-CMAQ. Following the cold front passage, $PM_{2.5}$ concentrations remained much lower in the FV3GFS-CMAQ throughout the entire depth of the PBL.

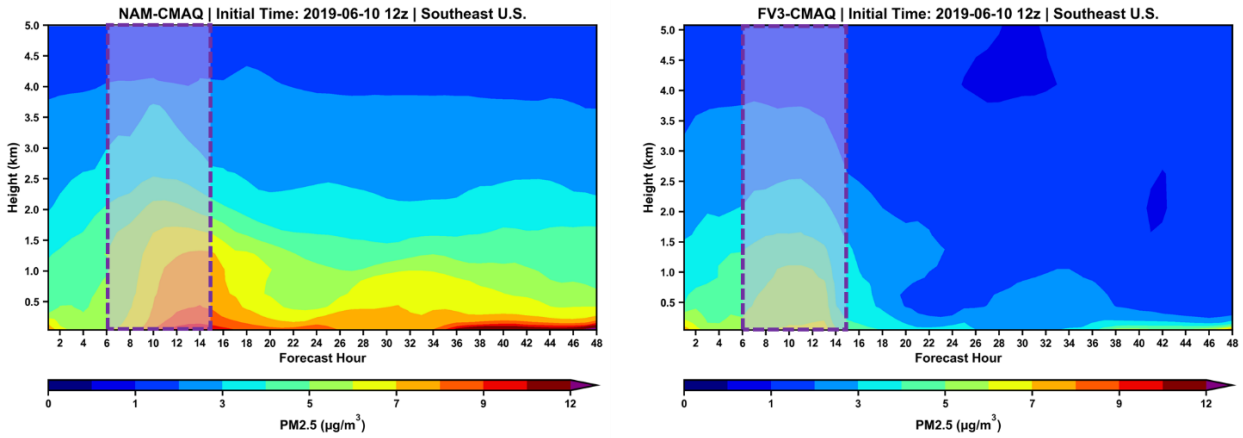

Figure 8. Hovmöller diagrams of height vs. forecast hour for the NAM-CMAQ (left) and FV3GFS-CMAQ (right) from 12 UTC on 10 June to 12 UTC on 12 June. The $PM_{2.5}$ concentrations range from dark blue (low) to dark red (high). The purple shaded areas approximate the cold front passage.

Chapter 4

Conclusions

This investigation evaluated and compared summertime $PM_{2.5}$ biases of the NAM-CMAQ and FV3GFS-CMAQ. Spatial maps of $PM_{2.5}$ concentrations over the CONUS domain show that the FV3GFS-CMAQ generally predicted less $PM_{2.5}$ than the NAM-CMAQ in the eastern United States. This means that using the FV3GFS-CMAQ over the NAM-CMAQ reduces $PM_{2.5}$ overprediction, but augments $PM_{2.5}$ underprediction. Regions with similar $PM_{2.5}$ biases in both models have errors in emissions, chemistry, or deposition that should be resolved through separate research efforts. In this study, we focused on an area with significant $PM_{2.5}$ bias discrepancies between the two models in order to scrutinize the reliability of numerical weather predictions incorporated in the NOAA-EPA NAQFC.

We found enhanced vertical mixing and nocturnal warming in the FV3GFS-CMAQ associated with a cold front passage traversing the Southeast on 11 June 2019, which is consistent with the findings of Hu et al. (2013). Our results confirm the speculation of Huang et al. (2018) that the FV3GFS eddy-diffusivity mass-flux PBL scheme is causing excessive mixing of $PM_{2.5}$ and contributing to the known $PM_{2.5}$ underprediction. This implies PBL height overprediction and greater removal of $PM_{2.5}$ by dry deposition. Notwithstanding, other removal mechanisms not investigated in this study could have been partially responsible for the $PM_{2.5}$ underprediction of the FV3GFS-CMAQ. Liu et al. (2019) emphasized the importance of

horizontal advection in synoptic wintertime $PM_{2.5}$ transport, and Wu et al. (2018) pointed to wet deposition as the predominant removal mechanism over wetlands in Beijing during summer.

To understand the relative contributions of advection, vertical mixing, and wet deposition, future work may include computing air parcel trajectories using the NOAA Hybrid Single Particle Lagrangian Integrated Trajectory (HYSPLIT) model and analyzing precipitation biases. Dry and wet deposition, as well as eddy diffusivity, would also provide further insight into the $PM_{2.5}$ prediction biases. The NAM-CMAQ probably has a more preferable PBL scheme and resolution over the FV3GFS-CMAQ in our case study, as underprediction may lead to greater $PM_{2.5}$ exposure. However, we need to look at additional synoptic patterns, different regions within CONUS, and consider other times of year before drawing firm conclusions. Future improvements in the FV3GFS will not only advance weather forecasts, but also contribute to more reliable air quality forecasts to help protect human health.

REFERENCES

AirNow API. *AirNow API Documentation*. Environmental Protection Agency (EPA). https://docs.airnowapi.org/

Brook, J. R., Poirot, R. L., Dann, T. F., Lee, P. K. H., Lillyman, C. D., & Ip, T. (2007). Assessing Sources of $PM_{2.5}$ in Cities Influenced by Regional Transport. *Journal of Toxicology and Environmental Health, Part A*, *70*(3-4), 191–199. doi:10.1080/15287390600883000

Chen, Z. H., Cheng, S. Y., Li, J. B., Guo, X. R., Wang, W. H., & Chen, D. S. (2008). Relationship between atmospheric pollution processes and synoptic pressure patterns in northern China. *Atmospheric Environment*, *42*(24), 6078–6087. doi:10.1016/j.atmosenv.2008.03.043

Hu, X.-M., Doughty, D. C., Sanchez, K. J., Joseph, E., & Fuentes, J. D. (2012). Ozone variability in the atmospheric boundary layer in Maryland and its implications for vertical transport model. *Atmospheric Environment*, *46*, 354–364. doi: 10.1016/j.atmosenv.2011.09.054

Hu, X.-M., Klein, P. M., Xue, M., Shapiro, A., & Nallapareddy, A. (2013). Enhanced vertical mixing associated with a nocturnal cold front passage and its impact on near-surface temperature and ozone concentration. *Journal of Geophysical Research: Atmospheres*, *118*(7), 2714–2728. doi:10.1002/jgrd.50309

Huang, J., McQueen, J., Wilczak, J., Djalalova, I., Stajner, I., Shafran, P., et al. (2017). Improving NOAA NAQFC $PM_{2.5}$ Predictions with a Bias Correction Approach. *Weather and Forecasting*, *32*(2), 407–421. doi:10.1175/waf-d-16-0118.1

Huang, J., McQueen, J., Shafran, P., Huang, H.-C., Kain, J., Tang, Y., et al. (2018, October 24). Development and evaluation of offline coupling of FV3-based GFS with CMAQ at NOAA. https://www.cmascenter.org/conference//2018/slides/1610_huang_development_evaluation_2018.pdf

Lee, P., Mcqueen, J., Stajner, I., Huang, J., Pan, L., Tong, D., et al. (2017). NAQFC Developmental Forecast Guidance for Fine Particulate Matter ($PM_{2.5}$). *Weather and Forecasting*, *32*(1), 343–360. doi:10.1175/waf-d-15-0163.1

Liu, Q., Chen, G., & Iwasaki, T. (2019). Quantifying the Impacts of Cold Airmass on Aerosol Concentrations Over North China Using Isentropic Analysis. *Journal of Geophysical Research: Atmospheres*. doi:10.1029/2018jd029367

Mesonet API. Synoptic Data PBC. https://developers.synopticdata.com/mesonet/

Mitchell, D. L., & Finnegan, W. (2009). Modification of cirrus clouds to reduce global warming. *Environmental Research Letters*, *4*(4). doi: 10.1088/1748-9326/4/4/045102

NAAQS Table. (2016, December 20). Environmental Protection Agency (EPA). https://www.epa.gov/criteria-air-pollutants/naaqs-table

Tsidulko, M., McQueen, J., Tassone, C., DiMego, G., Whiting, J., & Stajner, I. (2011, January 27). 91st American Meteorological Society Annual Meeting. *Evaluation of PBL depths for poor air quality episodes from the NOAA forecast systems (91st American Meteorological Society Annual Meeting)*. https://ams.confex.com/ams/91Annual/webprogram/Paper186888.html

Wang, J., & Ogawa, S. (2015). Effects of Meteorological Conditions on $PM_{2.5}$ Concentrations in Nagasaki, Japan. *International Journal of Environmental Research and Public*

Health, *12*(8), 9089–9101. doi:10.3390/ijerph120809089

Wang, Y.-jun, Xu, X.-de, Zhao, Y., & Wang, M.-Z. (2018). Variation characteristics of the planetary boundary layer height and its relationship with $PM_{2.5}$ concentration over China. *Journal of Tropical Meteorology*, *24*(3), 385–394. doi:10.16555/j.1006 8775.2018.03.011

Weber, R. J., Sullivan, A. P., Peltier, R. E., Russell, A., Yan, B., Zheng, M., et al. (2007). A study of secondary organic aerosol formation in the anthropogenic-influenced southeastern United States. *Journal of Geophysical Research: Atmospheres*, *112*(D13). doi:10.1029/2007jd008408

WPC Surface Analysis Archive. *Weather Prediction Center (WPC)*. National Oceanic and Atmospheric Administration (NOAA). https://www.wpc.ncep.noaa.gov/archives/web_pages/sfc/sfc_archive.php

Wu, Y., Liu, J., Zhai, J., Cong, L., Wang, Y., Ma, W., et al. (2018). Comparison of dry and wet deposition of particulate matter in near-surface waters during summer. *Plos One*, *13*(6). doi:10.1371/journal.pone.0199241

Zelle, H. (2012, January 9). Relative Humidity. *UCAR Mailman*. http://mailman.ucar.edu/pipermail/wrf-users/2012/002546.html

Zhang, R., Wang, G., Guo, S., Zamora, M. L., Ying, Q., Lin, Y., et al. (2015). Formation of Urban Fine Particulate Matter. *Chemical Reviews*, *115*(10), 3803–3855. doi:10.1021/acs.chemrev.5b00067

ACADEMIC VITA

BENJAMIN YANG

benjaminyang93@gmail.com

EDUCATION

The Pennsylvania State University — University Park, PA
Schreyer Honors College — 2016–2019
College of Earth and Mineral Sciences
Bachelor of Science, Meteorology and Atmospheric Science

RESEARCH INTERESTS

Numerical Weather Prediction, Planetary Boundary Layer, Atmospheric Dispersion, Ambient Air Quality, Atmospheric Chemistry, Land-Atmosphere Interactions, Mountain Meteorology, Satellite Data Assimilation, Artificial Intelligence

PROFESSIONAL EXPERIENCE

Research Intern, NOAA Environmental Modeling Center — Jun–Aug 2019
Diagnosed summertime $PM_{2.5}$ biases of the EPA Community Multiscale Air Quality Model. Provided novel model verification graphics and Python code to the air quality team. Launched an ozonesonde, conversed with NOAA and NASA scientists, and presented findings at the NOAA Center for Weather and Climate Prediction in College Park, MD.

Research Assistant, Penn State Department of Meteorology — Jan 2017–May 2019
Developed an algorithm with MATLAB to find PBL depths for B200 flights from the NASA Atmospheric Carbon and Transport-America winter 2017 campaign. Analyzed PBL depth variability across frontal boundaries using in-situ soundings and lidar.

Teaching Assistant, Penn State College of Earth and Mineral Sciences — Aug–Dec 2018
Assisted Dr. Michael Mann with teaching EMSC 100S: *Climate Change and Potential Societal Impacts*. Graded essays and helped students with their multimedia projects in office hours.

Research Intern, WSU Laboratory for Atmospheric Research May–Aug 2018
Evaluated three WRF model simulations for an active wildfire period. Toured the Pacific Northwest National Laboratory and presented poster at the Summer Undergraduate Research Symposium at Washington State University.

Researcher, Universidad San Ignacio de Loyola May 2018
Participated in The GREEN Program. Assessed the sources and effects of the Huatanay River's pollution, conducted a field experiment to model water flow through aqueducts, and made renovations in a village to improve water quality. Spearheaded a capstone project on the relationship between climate change and hydropower in Peru.

Learning Assistant, Penn State Department of Chemistry Aug–Dec 2017
Assisted Dr. Mary Bojan with teaching CHEM 110: *Chemical Principles I*. Coached over 200 students in lecture, taught problem-solving skills in recitation, proctored exams, and directed weekly review sessions.

PUBLICATIONS & PRESENTATIONS

Yang, B., Huang, J., McQueen, J. (2020). Diagnosing Summertime $PM_{2.5}$ Biases of the CMAQ Model Driven by the FV3GFS. *Accepted abstract for oral presentation* at the 100th Annual AMS Annual Meeting. Boston, MA.

Yang, B., Huang, J., McQueen, J. (2019). Diagnosing Summertime $PM_{2.5}$ Biases of the CMAQ Model Driven by the FV3GFS. *Paper in preparation.*

Yang, B., Huang, J., McQueen, J. (2019). Diagnosing Summertime $PM_{2.5}$ Biases of the CMAQ Model Driven by the FV3GFS. *Oral presentation* at the National Centers for Environmental Prediction Student Presentation Workshop. College Park, MD.

Yang, B., Ravi, V., Vaughan, J., Lamb, B., Lee, Y. (2019). Evaluation of Three Numerical Weather Predictions Using the Weather Research and Forecasting Model. *Poster presentation* at the 18th Annual AMS Student Conference. Phoenix, AZ.

Yang, B., Ravi, V., Vaughan, J., Lamb, B., Lee, Y. (2018). Evaluation of Three Numerical Weather Predictions Using the Weather Research and Forecasting Model. *Poster presentation* at the EMS Undergraduate Poster Exhibition. University Park, PA.

Yang, B., Ravi, V., Vaughan, J., Lamb, B., Lee, Y. (2018). Evaluation of Three Numerical Weather Predictions Using the Weather Research and Forecasting Model. *Poster presentation* at the WSU Summer Undergraduate Research Symposium. Pullman, WA.

HONORS & AWARDS

EMSAGE Laureate	2019
Science Systems and Applications, Inc. AMS Scholarship	2019
John K. Tsui Honors Scholarship	2019
John T. Ryan Jr. Scholarship in Earth and Mineral Sciences	2018, 2019
Robert O. Cole Scholarship in Meteorology	2018, 2019
Chi Epsilon Pi Meteorology Honor Society	2018–2019
Academic Excellence Scholarship	2016–2019
Dean's List	2016–2019
Penn State Meteorology Photo Contest Third Place Winner	2018
GREEN Program EMS Scholarship	2018
Schreyer International Study & Conference Travel Grants	2018
Charles L. and Anna R. Hosler Scholarship in Meteorology	2017
Penn State Alumni Association - Puget Sound Chapter Scholarship	2017
NASA Pennsylvania Space Grant First-Year Undergraduate Research Scholarship	2017
Matthew J. Wilson Honors Scholarship	2016, 2017
Dean's Freshman Scholarship in Meteorology	2016

OTHER ACTIVITIES

Forecasting Shift Manager, Penn State Campus Weather Service	Aug 2017–Dec 2019
President, Penn State Lutheran Student Community	Jan 2018–Dec 2019
Penn State Club Cross Country	Aug 2016–Dec 2019
The GLOBE - Honors Special Living Option	Aug 2016–May 2019
Penn State Concert & Campus Bands	Aug 2016–May 2019
Treasurer, Penn State Chi Epsilon Pi Meteorology Honor Society	Apr 2018–Apr 2019
Webmaster, Penn State Storm Chase Team	Sep 2017–May 2018
Mentor, First-Year Schreyer Honors Orientation	Jan 2017–Sep 2017
Exhibit Floor Volunteer, Discovery Space Museum	Sep 2016–May 2017